Nonlinear Properties of Traveling-Wave Electroabsorption Modulator

Jongin Shim, *Member, IEEE*, Bin Liu, Joachim Piprek, *Senior Member, IEEE*, and John E. Bowers, *Fellow, IEEE*

Abstract—We report the nonlinear properties of traveling-wave electroabsorption modulators experimentally and theoretically. The saturation characteristics of the dc transfer curve give rise to the superlinear, linear, and sublinear properties of output signal levels against the input signal levels. The dynamic behavior of the transmission curves for a wide range of the input radio-frequency signal levels can be described using the dc transfer curve and the fast Fourier transform algorithm.

Index Terms—Electroabsorption modulator (EAM), nonlinearity, saturation, transfer curve.

I. INTRODUCTION

IN ANALOG fiber-optic links, semiconductor multiple quantum-well traveling-wave electroabsorption modulators (TWEAMs) have been widely studied due to their small size, large bandwidth, low driving voltage, and potential for monolithic integration with laser and amplifier [1], [2]. Spurious-free dynamic range (SFDR), link gain (G), and noise figure are the main figures of merit that quantify the analog performances of the device [2]. The experimental results tend to agree with the theoretical ones for low input radio-frequency (RF) powers. However, nonlinear performance at high RF driving power is more complicated.

SFDR is often calculated by assuming that the fundamental signal linearly increases with the input RF signal with a slope of one [3]. This is true if the input RF power is sufficiently low. However, with increasing input RF power (modulation depth), the output RF signal power saturates. The output RF power corresponding to the 1-dB output compression point is commonly used as the saturation power [4]. The slope of the output RF signal power against the input signal power n depends on the bias and RF input signal level. The G is mainly determined by the slope efficiency at the bias point of the transfer curve based on the small signal analysis. G is independent on the input signal level for a small signal power. However, G depends not only on the bias point but also on input power level in the case of a high input signal power. The dependence of G on the input signal power level will be clarified in this letter. The harmonic distortion generated by the nonlinear transfer characteristic has been usually analyzed by expanding the transfer function to the

J. Shim is with the Department of Electrical and Computer Engineering, University of California, Santa Barbara, CA 93106 USA, on leave from the Department of Electrical and Computer Engineering, Hanyang University, Kyungki-do 425-791, Korea (e-mail: jishim@giga.hanyang.ac.kr).

B. Liu, J. Piprek, and J. E. Bowers are with the Department of Electrical and Computer Engineering, University of California, Santa Barbara, CA 93106 USA.
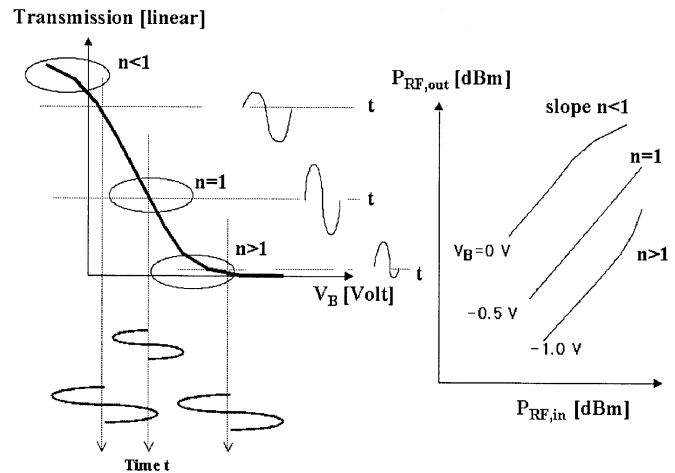
Fig. 1. Schematic plot of the relation between RF input and output powers for three different bias voltages in the TWEAM.

power series around the operating point [5]. This method is very effective when the input signal level is low. However, the power series expansion method is not sufficient when the input signal level is large.

In this letter, the dependence of the RF signal output power on the RF input power in the TWEAM is investigated experimentally and theoretically. We clarify the dependence of signal characteristics on input power levels by using transfer curve and large signal analysis based on the fast Fourier transform (FFT) algorithm.

II. DEVICE STRUCTURE AND ANALYSIS METHOD

The TWEAM structure described herein is the same as reported previously [6]. The active layers consist of 10 tensile-strain wells (InGaAsP, 0.35%, 12 nm) and 11 compressive-strain barriers (InGaAsP, 0.57%, 7 nm), embedded in a ridge waveguide. The modulator length is 300 μm and the ridge width is 2 μm. The facets are coated by antireflection films. The termination load for the microwave signal is an open circuit. The 3-dB bandwidth for open termination is about 10 GHz. A high-power tunable laser is used as the input optical source. The lasing wavelength is set to 1.555 μm with transverse-electric polarization. Two lensed fibers are used to couple light into the electroabsorption modulator (EAM) and the photodetector. The total coupling loss is 6 dB. The device is mounted on the copper block.

Fig. 1 shows the schematic transfer characteristic for the bias voltage and RF input power. In the figure, three cases are illustrated. For a bias in the center of the linear range, linear response is expected. For biases to the edge of the linear region,
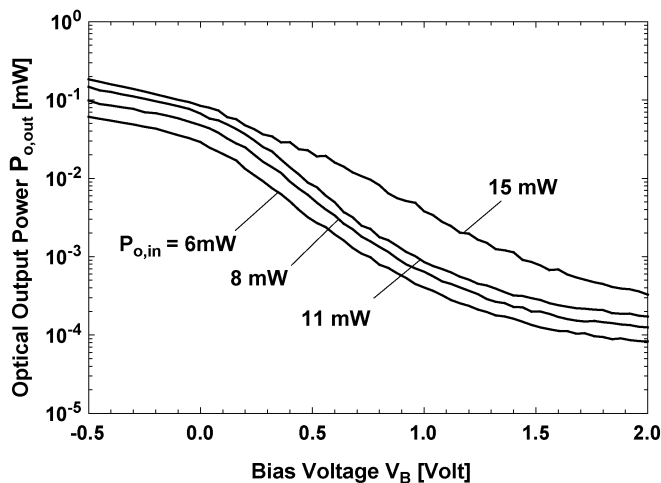
Fig. 2.   Optical transmission versus bias with the optical input power as parameter.
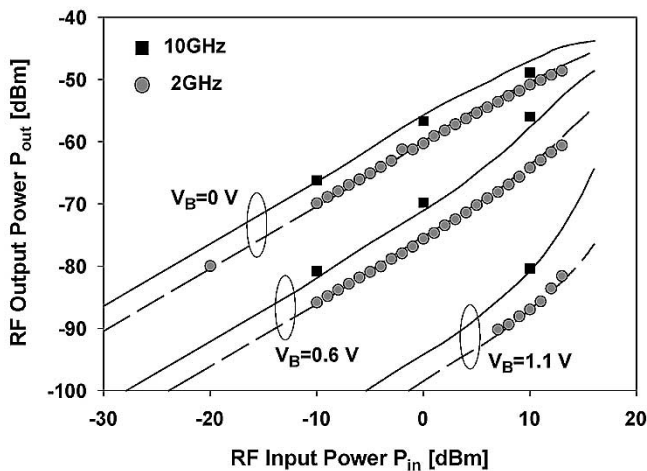

Fig. 3.   Experimental results of RF output powers for the different operating conditions.

sublinear response is expected. For a bias above the linear region, superlinear response is expected. In order to analyze the ac performance, we assume that the dc transfer curve is directly applicable to simulate ac signal performances if the signal frequency is less than 3-dB bandwidth. In the theoretical analysis, a sinusoidal RF input voltage is assumed around the bias voltage and the FFT algorithm is used. The microwave loss—including cable loss—and the reflection loss are estimated to be 6 and 8 dB at 10 GHz, respectively.

III. RESULTS AND DISCUSSIONS

Fig. 2 shows optical output power transmitted through the EAM. The small signal optical output power after the modulator is proportional to the first derivative of the transfer curve. The relation between RF output power and RF input power is linear for small driving voltages. However, the transfer curve is not linear in the case of high input RF power. In the following experiment, we set the input optical power as high as 8 mW. Fig. 3 shows the dependence of the RF signal output power on RF input power
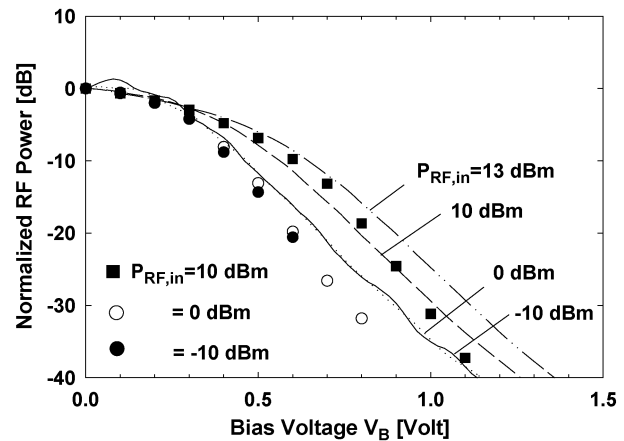

Fig. 4.   RF output powers normalized to the values at zero bias voltage $V_B = 0$ V for the different RF input powers. The dotted points and the lines represent the experimental and theoretical data, respectively.

for several bias voltages. The lines correspond to calculated results and the points are measured. The theoretical curves show good agreement with the experiments. This indicates that the dc transmission curve can be used to explain nonlinear effects of TWEAMs, provided that the input RF signal frequency is less than the bandwidth of the eletrooptical response. The analysis explained that the frequency dependences shown in Fig. 3 result from the difference of microwave reflection loss of about 4 dB between two frequencies in our measurement setup. When the input signal power is less than about 0 dBm, the output signal power is linearly proportional to the input power regardless of bias voltages. However, when the bias voltages are as small as 0 V or as large as 1.1 V, sublinear (slope = $n < 1$) or superlinear ($n > 1$) curves are clearly observed for large input RF powers, respectively. These are due to the nonlinear effects of the transfer curves for the operating voltage regions. A more linear output signal against input signal RF power can be expected by setting bias voltage at a slightly larger value than 0 V. With 9-dBm optical input power, the RF-to-RF gain G is only about −55 dB for 10 GHz signal frequency. This is due to the high optical loss of −20.5 dB (12 dB for coupling loss and 8 dB for transmission loss) and the microwave loss of 14 dB (6 dB for cable loss and 8-dB reflection loss). These losses can be greatly reduced by using a high optical coupling scheme, low loss microwave cable, and microwave impedance matching circuits [7].

Fig. 4 shows the output RF power normalized to the zero bias point according to the bias voltage for different input RF powers. The dots and the straight lines correspond to the experimental and the theoretical values, respectively. When the RF input power is very small, the small signal analysis is reasonably accurate, and the RF gain is determined by the slope efficiency at the bias voltage, which is independent of RF input power. Thus, the normalized output power curves for $P_{\text{RF,in}} = -10$ and 0 dBm have the same shape. However, for large input signal RF power, both the theoretical and experimental results show that the normalized output value increases for higher bias voltage. This is because the modulator RF output power is mainly determined by the maximum transmitted optical power that is proportional to the peak voltage of RF signal applied to TWEAM. Thus, it is clear that
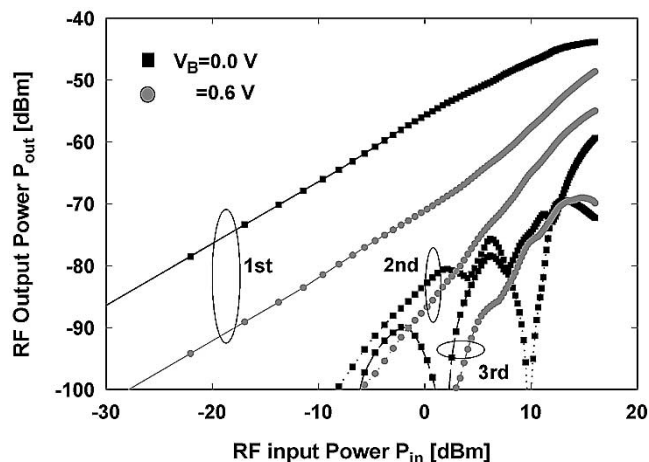
Fig. 5.   Calculated harmonic distortions of the TWEAM as a function of RF input power.

the RF-to-RF gain is determined by the first-order Fourier component of the modulated signal in the photodetector which can be predicted only by the large signal analysis.

In order to achieve maximum RF signal output power, it is necessary to apply both high optical input power $P_{opt,in}$ and high RF input power. The transfer curves in an EAM strongly depend on the optical input power, as shown in Fig. 2, which is mainly due to the band-filling effect in the quantum well as well as the increase of device temperature with the photocurrent [8]. It is found, experimentally, that the dependence of RF signal gain on the bias voltage is much stronger at low input optical power than at high input optical power. The maximum RF gains are achieved at the bias voltages of $0 \text{ V} < V_B < 0.5 \text{ V}$ for $P_{opt,in} < 10$ dBm and $V_B > 0.5$ V for $P_{opt,in} > 10$ dBm [7].

Nonlinearity of the transfer curve in a TWEAM produces harmonic distortions. Fig. 5 shows the calculated values of harmonic distortions at the input RF signal frequency of 10 GHz at two bias voltages of 0.0 and 0.6 V. The output signal frequencies of the second and the third harmonic signals correspond to 20 and 30 GHz, respectively. If the applied RF input power is small enough that the first-order signal increases with the RF input power by the slope of one, the second- and the third-order harmonic signal powers increase with the slope of two and three, respectively. In this range of the input RF power, the op-

erating conditions for the minimum nonlinear distortions can be found by applying the small signal analysis. Thus, the minimum second and third harmonic distortions can be realized by biasing EAMs at the points where the second and third derivatives are zero in the transfer curves, respectively. However, when the input RF power is so large that the first-order signal power does not increase with the slope of one, the higher order harmonic distortions also become highly nonlinear. Therefore, harmonic distortions should be examined by the large signal analysis and their values would be determined by the Fourier components of the modulated signal.

IV. CONCLUSION

The nonlinear properties of TWEAM for the several different operating conditions have been studied experimentally and theoretically. It was clarified that the dc transmission curve can be used to explain the nonlinear effects of TWEAMs. The saturation characteristics of the dc transfer curve gave rise to the superlinear, linear, and sublinear properties of output signal levels against the input signal levels. Furthermore, it was shown that the dependence of the normalized ac transmission curves on RF input power was caused by the nonlinear properties of the dc transfer curve.

REFERENCES

[1] S. Kaneko, M. Node, Y. Miyazaki, H. Watanabe, K. Kasahara, and T. Tajime, "An electroabsorption modulator module for digital and analog applications," *J. Lightwave Technol.*, vol. 17, pp. 669–676, Apr. 1999.

[2] W. S. C. Chang, *RF Photonics Technology in Optical Fiber Links*.   Cambridge, U.K.: Cambridge Univ. Press, 2002.

[3] G. E. Betts, C. H. Cox III, and K. G. Ray, "20 GHz optical analog link using an external modulator," *IEEE Photon. Technol. Lett.*, vol. 2, pp. 923–925, Dec. 1990.

[4] T. Olson, "An RF and microwave fiber-optic design guide," *Microw. J.*, vol. 39, no. 8, pp. 54–78, 1998.

[5] D. D. Henkes and S. C. Kwok, "Intermodulation: Concepts and calculation," *Appl. Microw. & Wireless*, vol. 9, pp. 38–42, July/Aug. 1998.

[6] Y. Chiu, V. Kaman, S. Z. Zhang, and J. E. Bowers, "Distributed effects model for cascade traveling-wave electroabsorption modulator," *IEEE Photon. Technol. Lett.*, vol. 13, pp. 791–793, Aug. 2001.

[7] Z. Bian, J. Christofferson, A. Shakouri, and P. Kosedoy, "High power operation of electroabsorption modulators," in *Conf. Dig., CLEO/QELS 2003*, Baltimore, MD, 2003, Paper CtuJ5.

[8] B. Liu, J. Shim, Y. Chiu, A. Keating, J. Piprek, and J. Bowers, "Analog characterization of low-voltage MQW traveling-wave electroabsorption modulators," *J. Lightwave Technol.*, vol. 21, pp. 3011–3019, Dec. 2004.